Algorithm Applications in Robotic Planetary Exploration

Brent J. Bos
NASA Goddard Space Flight Center

Information Science & Technology Colloquium Series
September 30, 2009

Outline

I. Mars Pathfinder Image Processing (1997)

II. Phoenix Mars Lander Camera Operations (2008)

III. Future Planetary Instrument Data Compression Algorithm (Present)

IV. Summary

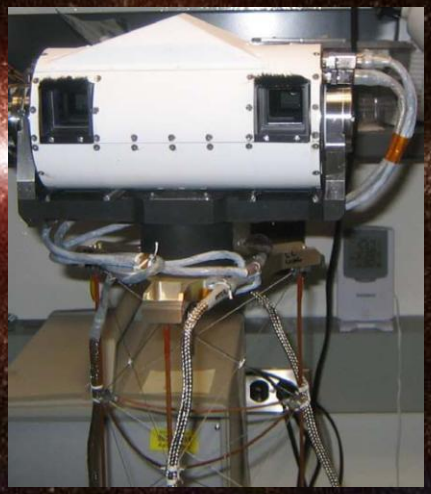

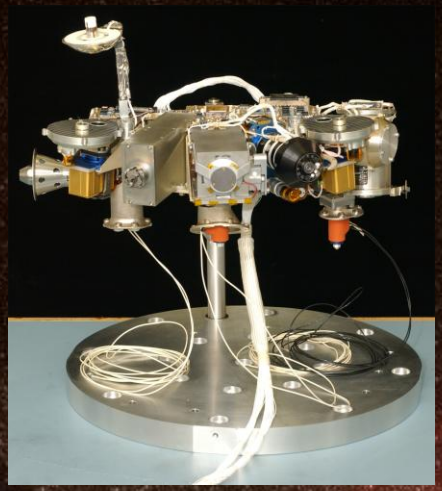

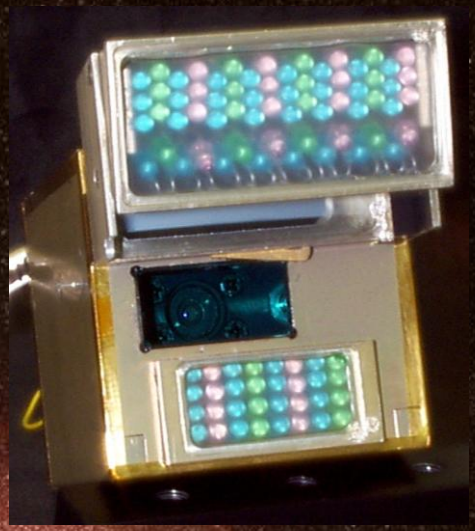

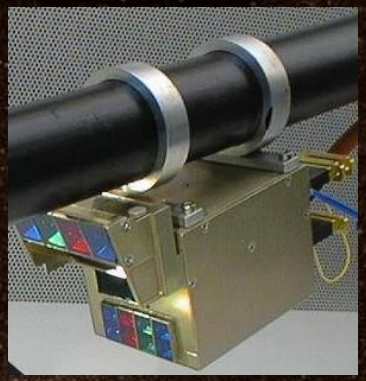

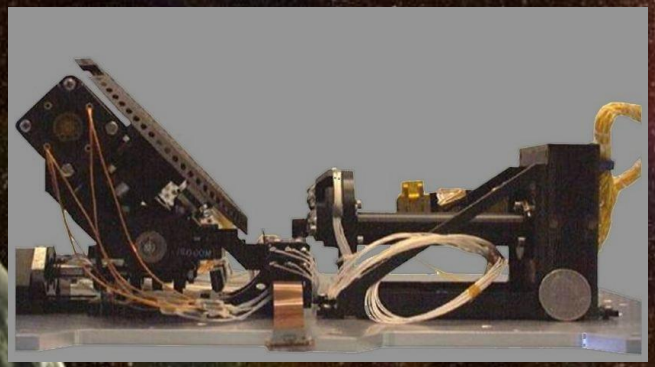

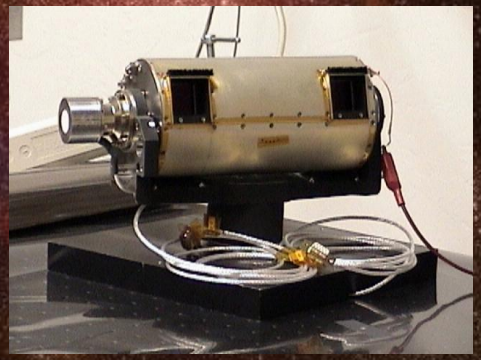

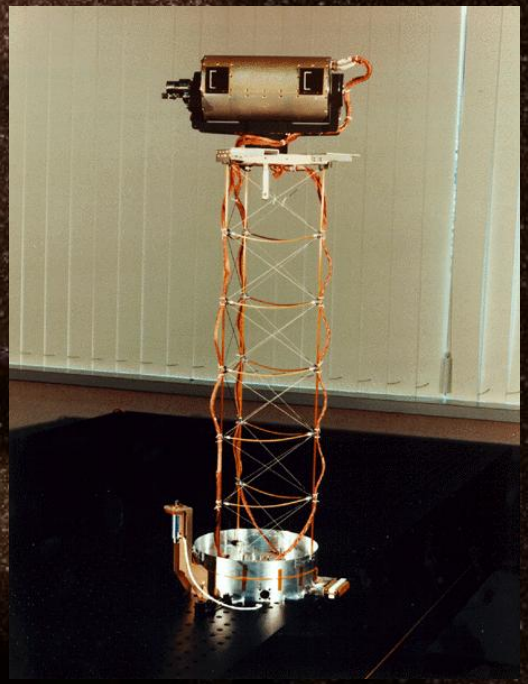

Linear System Imaging Theory

Image we got

Image we want

$$I(x,y) = \left[PSF_{sys}(x,y) ** I_0(x,y)\right] \cdot \frac{1}{|P^2|} comb\left(\frac{x}{P}, \frac{y}{P}\right) \cdot rect\left(\frac{x}{W_x}, \frac{y}{W_y}\right)$$

2D Convolution Blurs the Image

Sampling by Detector
P = pixel pitch

Image extent limited by Detector widths
W_x, W_y

$$PSF_{sys} = PSF_{lens} ** PSF_{CCD}$$

Degraded from a delta function by diffraction and lens aberrations

Determined by pixel width and pixel crosstalk (charge diffusion, substrate transparency, read-out noise, etc.)

$$PSF_{CCD}(x, y) = \sum_{i=1}^{9} R_i \; rect\left(\frac{x-x_i}{b_x}\right) rect\left(\frac{y-y_i}{b_y}\right)$$

For 100% fill-factor detectors: $b_x = W_x$, $b_y = W_y$

$$rect\left(\frac{x-x_o}{b}\right) = \begin{cases} 0, & \left|\frac{x-x_o}{b}\right| > \frac{1}{2} \\ \frac{1}{2}, & \left|\frac{x-x_o}{b}\right| = \frac{1}{2} \\ 1, & \left|\frac{x-x_o}{b}\right| < \frac{1}{2} \end{cases}$$

Mars Pathfinder Deconvolution

In practice, taking advantage of the Fourier domain typically does not work due to noise in the image.

$$I_0(x,y) = F^{-1}\left[\frac{F\left[I(x,y)\right]}{F\left[PSF_{sys}(x,y)\right]}\right]$$

Instead, iterative deconvolution techniques (*Richardson-Lucy*) are employed using various assumptions for the image noise.

"Forward" process where I_0 are tried until the convolved image matches the final image, I.

$$I(x,y) = \left[PSF_{sys}(x,y) ** I_0(x,y)\right] \cdot \frac{1}{|P^2|} comb\left(\frac{x}{P}, \frac{y}{P}\right) \cdot rect\left(\frac{x}{W_x}, \frac{y}{W_y}\right)$$

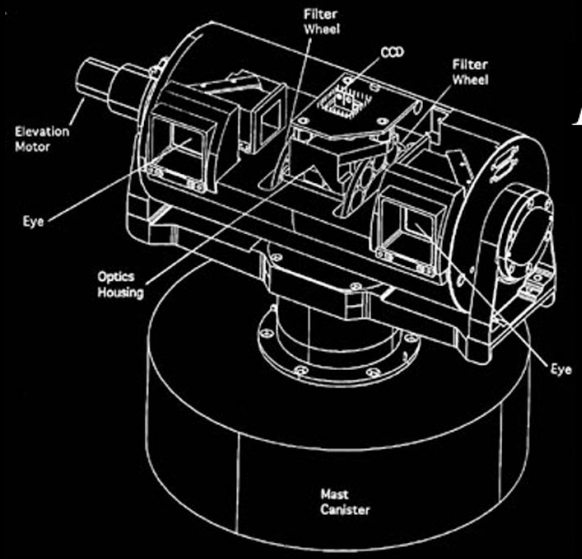

$$I(x,y) = \left[PSF_{sys}(x,y) ** I_0(x,y)\right] \cdot \frac{1}{|P^2|} comb\left(\frac{x}{P}, \frac{y}{P}\right) \cdot rect\left(\frac{x}{W_x}, \frac{y}{W_y}\right)$$

Effectively smaller pixel pitches (*P*) were achieved by taking multiple images at random positions of the IMP's azimuth motor, correct image-to-image positioning achieved using image correlation.

Sometimes called "Super-Resolution"

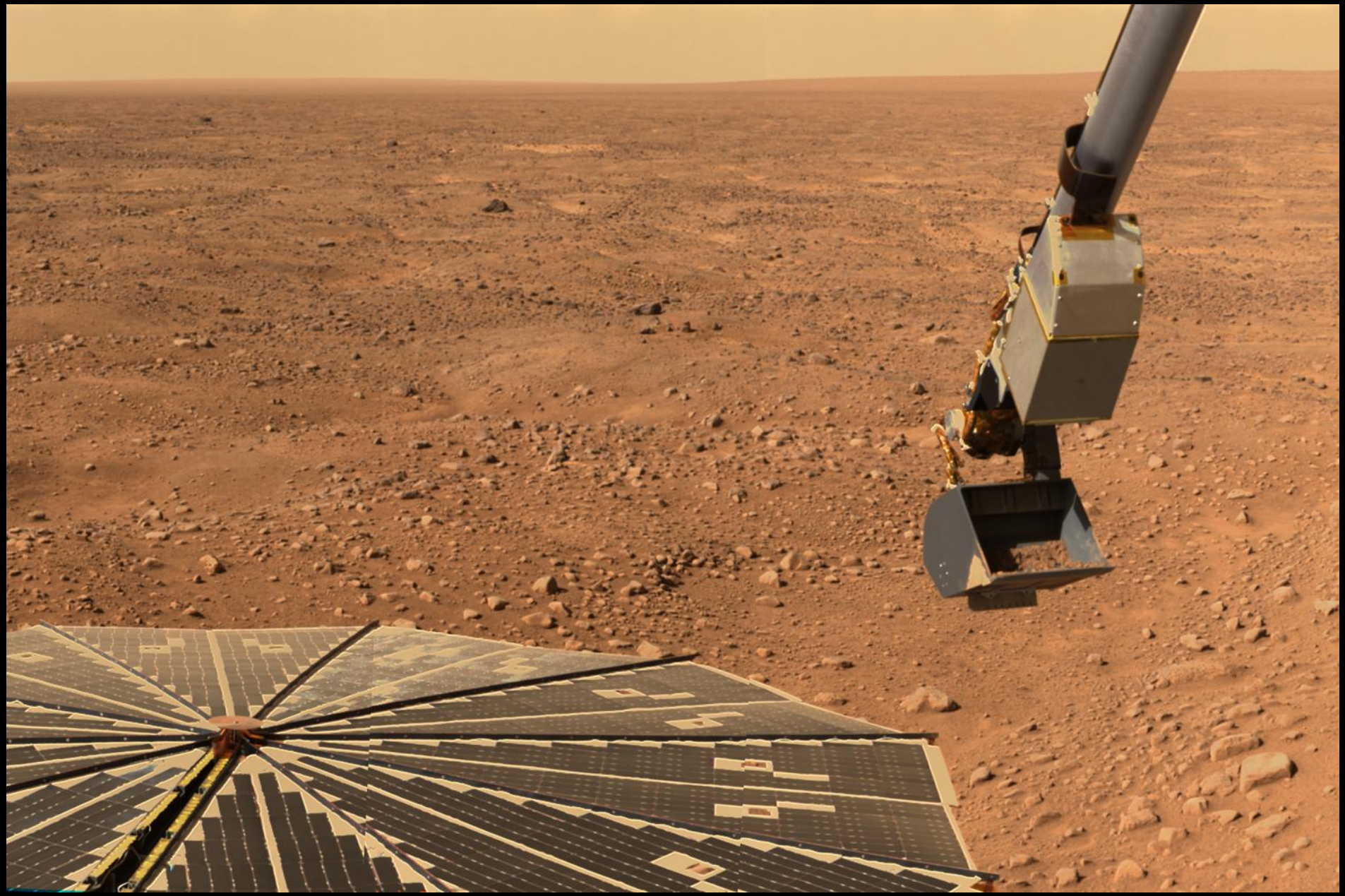

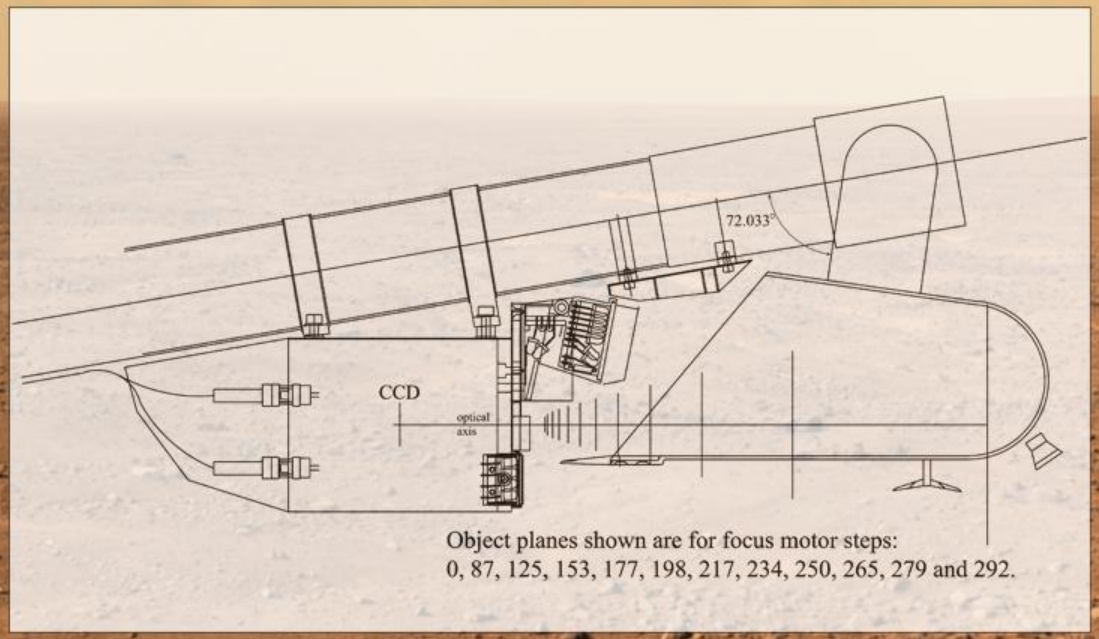

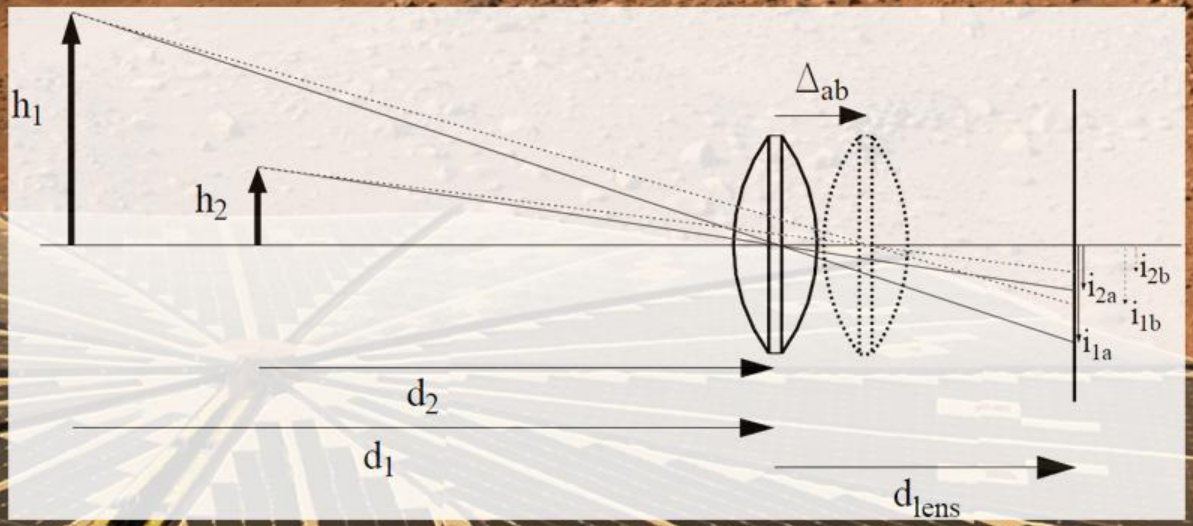

$$\frac{i_{1b}}{i_{2b}} = \frac{h_1 (d_2 + \Delta_{ab})}{h_2 (d_1 + \Delta_{ab})}$$

Depth of Focus Algorithm Overview

Increase image scale by cubic convolution for each image in the focus series, relative to the image acquired at the lowest focus motor step.

All images in focus cube linearly scaled to generate correct relative image scale at highest resolution focus

Normalize each image to 1.

High pass filter each image and square result.

$$F_1 = \sum_{i,j} \left(\begin{bmatrix} -1 & -2 & -1 \\ -2 & 12 & -2 \\ -1 & -2 & -1 \end{bmatrix} ** g_{i,j} \right)^2$$

Average each high pass filtered image with circular window to create strength of focus map.

Assemble strength of focus map into cube *m(x,y,z)* where *z* is the lens position.

Determine which pixels in the focus cube have the strongest focus signal

Determine strength of focus threshold by binning all strength of focus values (512x256x# focus steps), threshold is set so that 512x256x1.25 pixels are above threshold.

Create 512x256 in-focus image *i(x,y)* and in-focus map *mi(x,y)*.

Begin assembling single in-focus image based on focus map

Assign values to *i(x,y)* and *mi(x,y)* based on which position *z* in *m(x,y,z)* has the strongest focus, is above the threshold and has at least 41 pixels from the same *z* in a 9x9 window.

Unassigned pixels in *i(x,y)* and *mi(x,y)* are chosen through recursive region growing, initially 8 connectedness is required but is reduced to fill *mi(x,y)*, multiple classification is resolved based on strongest focus.

Assign pixels with ambiguous in-focus signals to in-focus image using region growing with iteratively reducing connectedness threshold

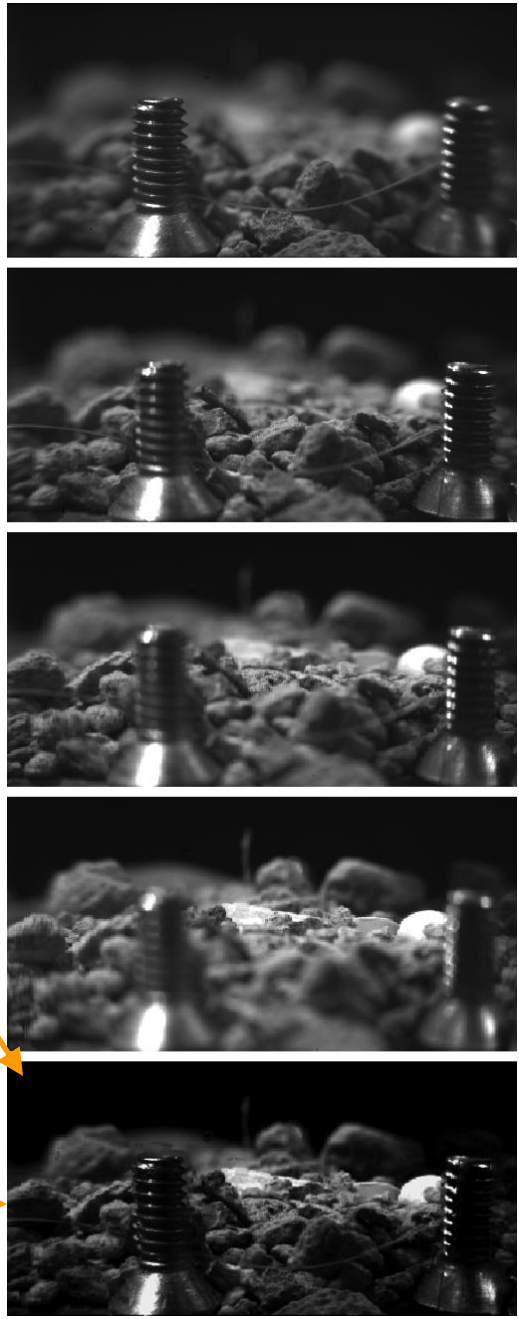

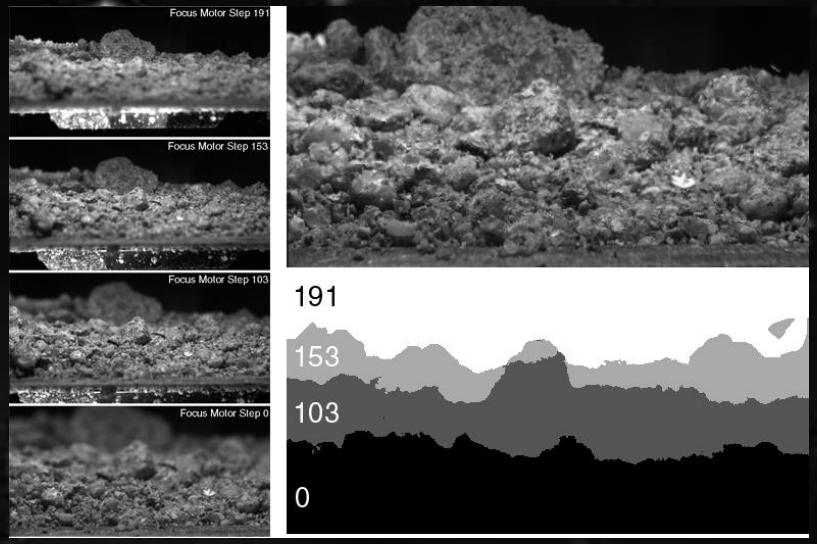

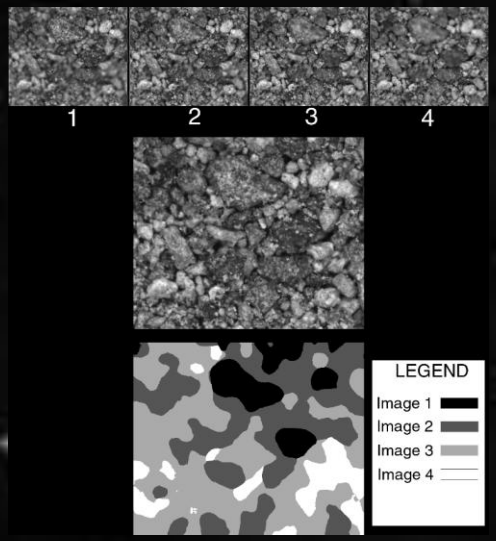

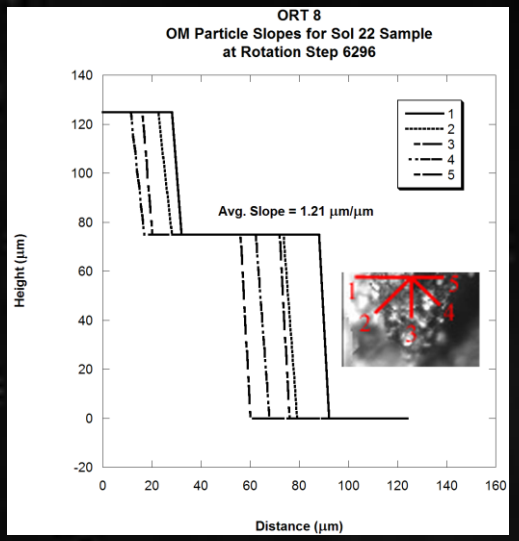

Original motivation for development was as a lossy but high-fidelity image compression algorithm – processing time concerns and calibration uncertainty kept it from being used in that manner.

Ended up being used as an image/scene analysis tool and a tool for quick follow-on imaging decisions.

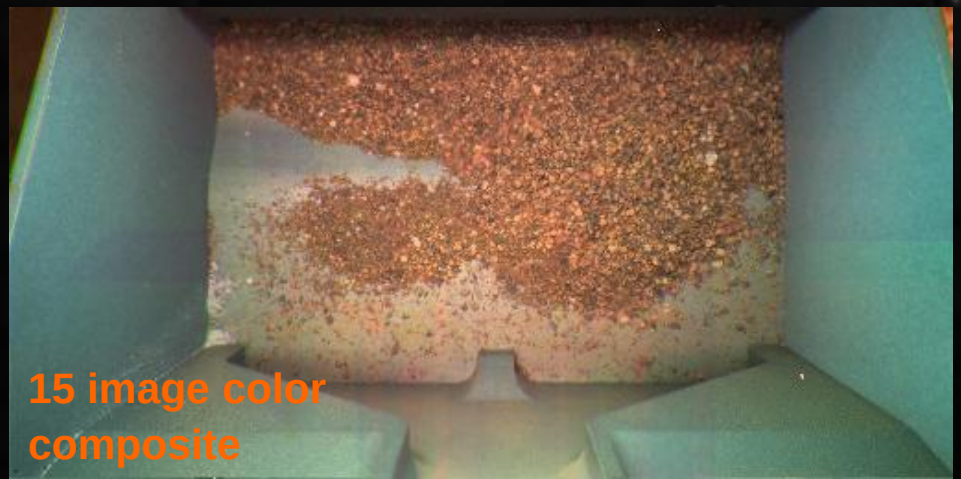

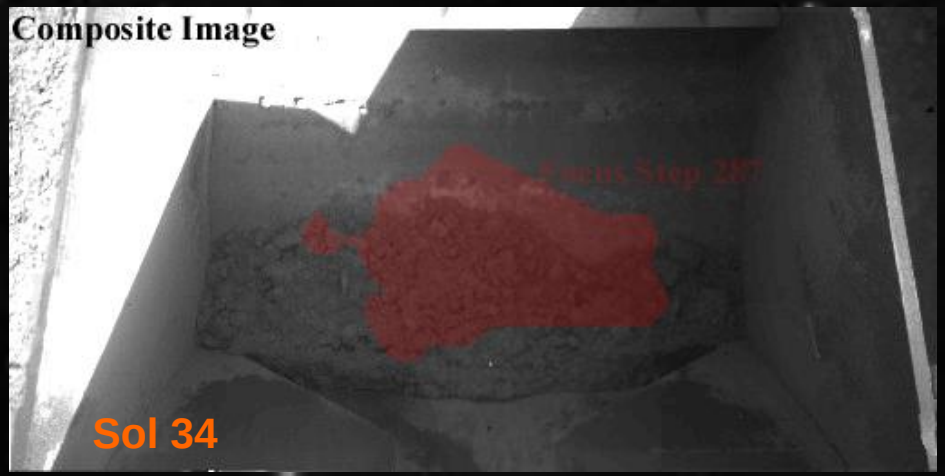

Planetary Dust Characterization Instrument

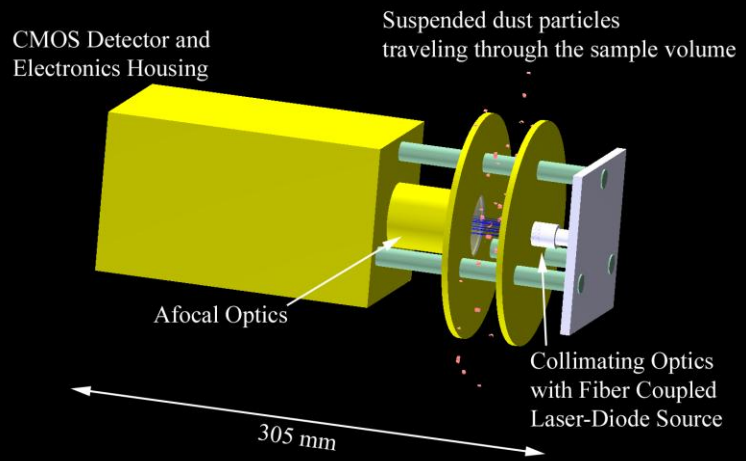

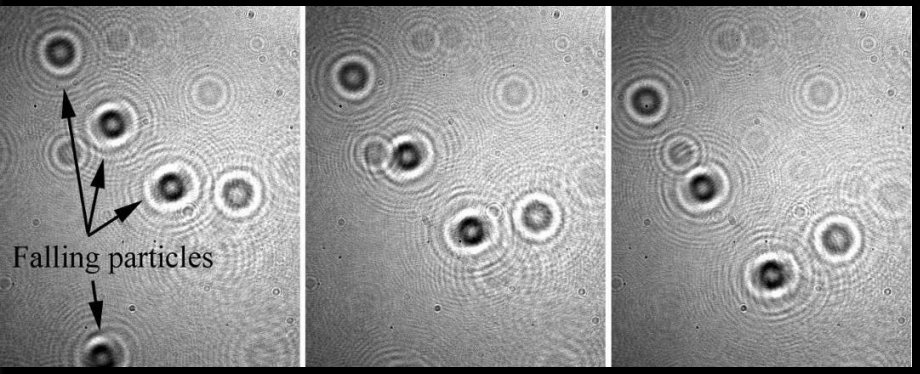

- **Large depth-of-field particle image velocimeter (PIV) measures suspended dust particle size, shape, flux, number density and velocity (speed and direction) on planetary surfaces.**
- **To measure dynamic dust activity, high frame rates (4000 Hz) are required → generating >1 TB for every event.**
- **Developing an algorithm to reduce the data by more than 10^3 before downlink.**

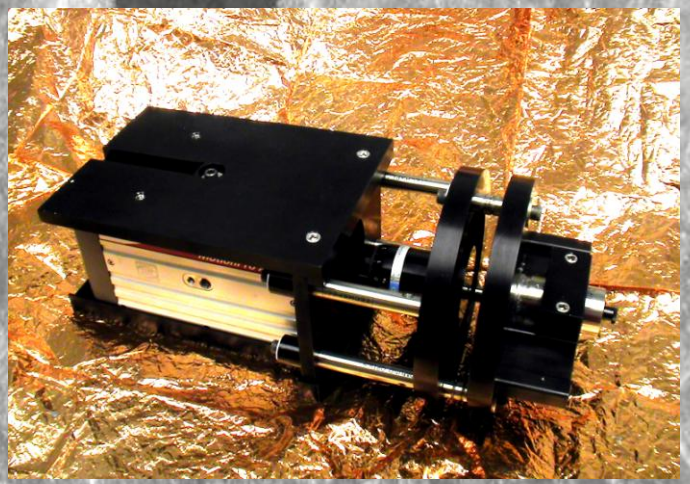

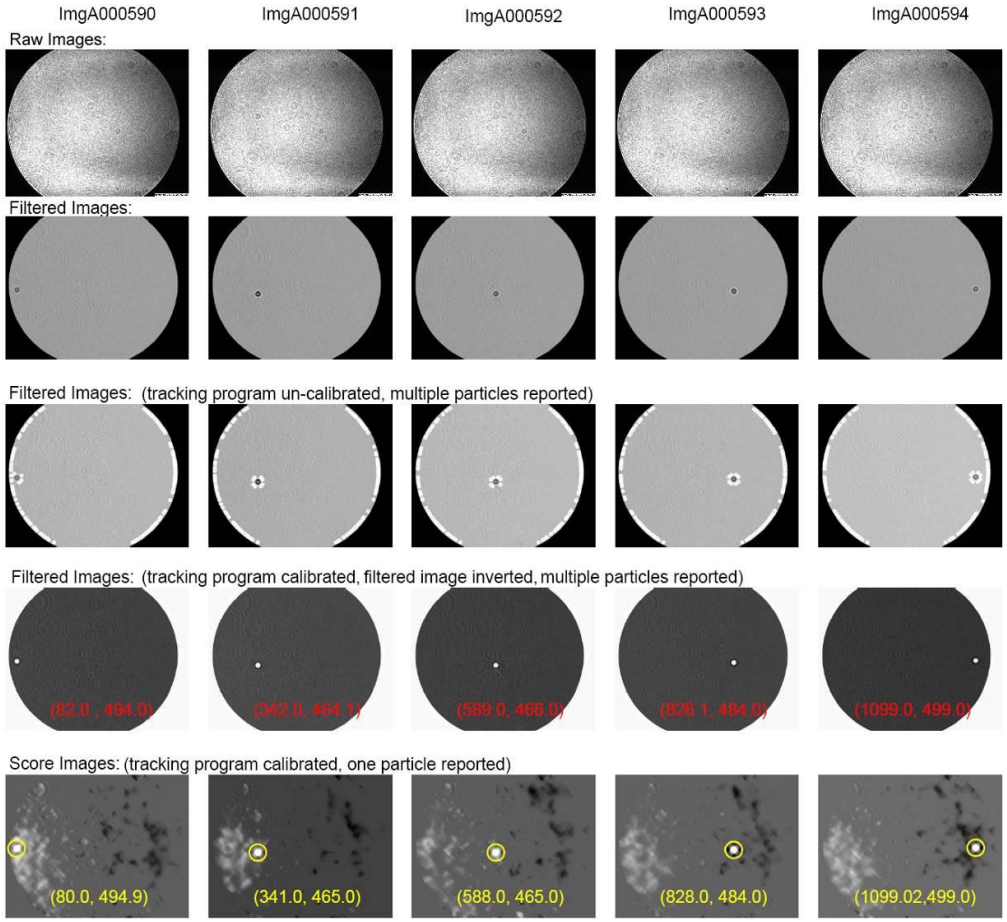

Algorithm Processing of PIV data from a June 3, 2007 dust cyclone intercept

PIV Data Compression Algorithm Architecture

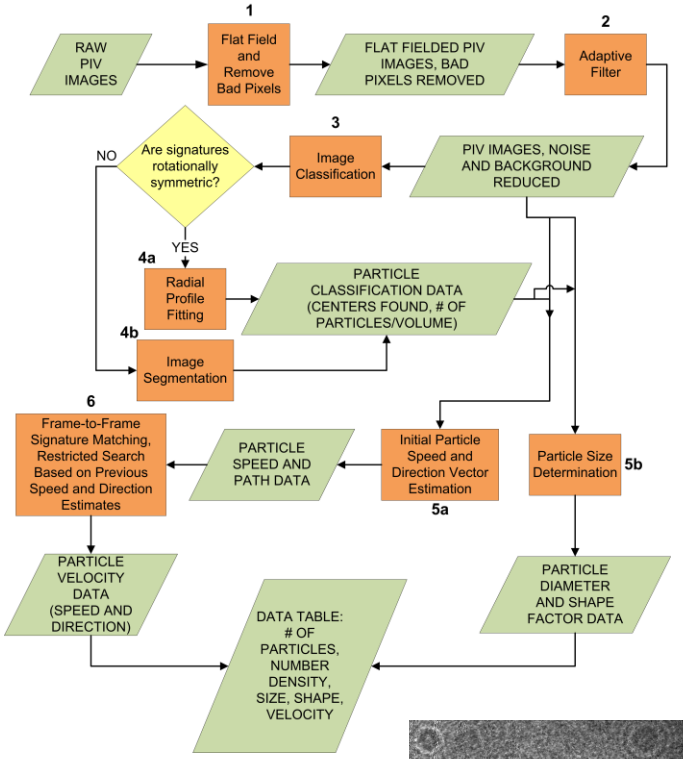

RAW PIV Image

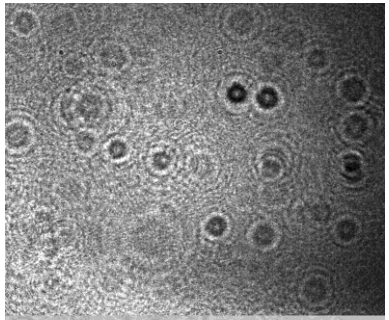

Image after Steps 1 and 2

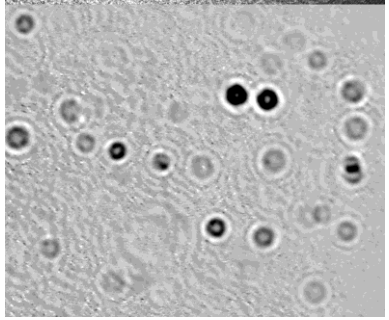

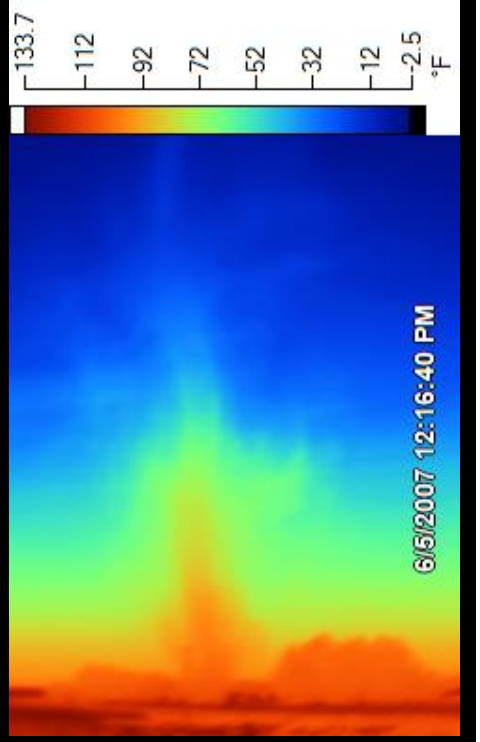

Algorithm processing of June 5, 2007 dust cyclone PIV data

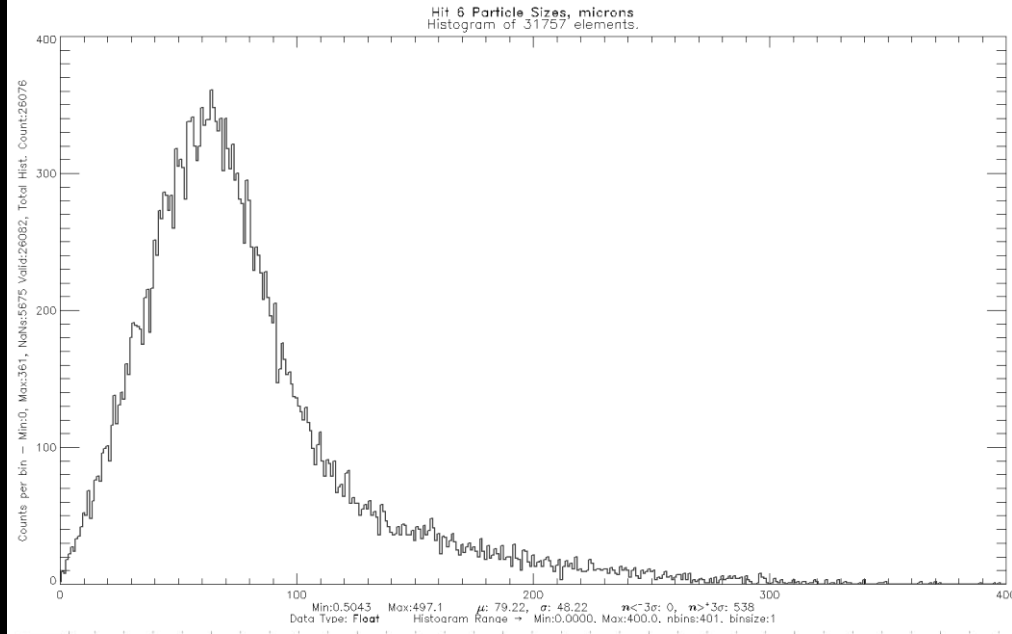

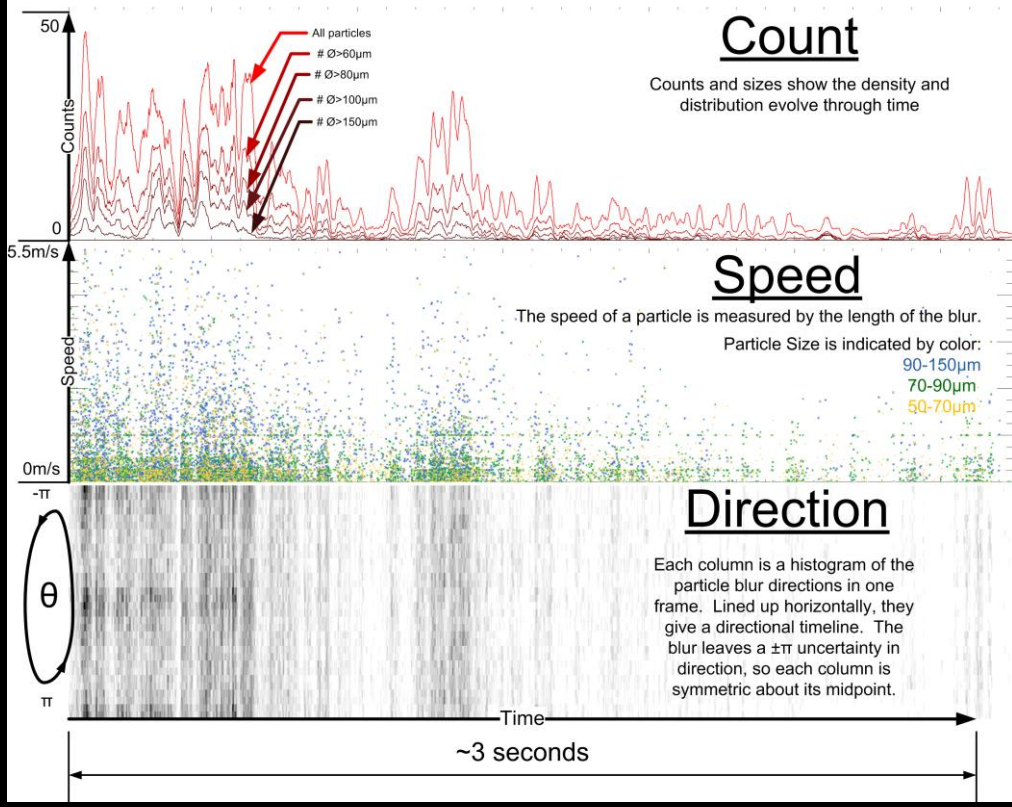

Summary

- Robotic planetary lander missions can benefit greatly from the application of advanced image processing algorithms
  - Improve real time response to data/decision making
  - Enhance scientific return
- Since NASA's 1997 return to the surface of Mars, advanced image processing algorithms have been used on all Mars lander missions
  - Mars Pathfinder: stereo imaging/ranging, hazard avoidance, super resolution...
  - Mars Exploration Rovers: stereo imaging/ranging, hazard avoidance, dust cyclone hunting, particle classification...
  - Phoenix Mars Lander: stereo imaging/ranging, deconvolution, depth of focus, particle classification...
- As spacecraft computers become more powerful (and/or FPGA technology matures), development of more onboard algorithm logic will be a priority (*e.g.* PIV data compression)